

ART: Adaptive Resampling-based Training for Imbalanced Classification

Arjun Basandrai*

Shourya Jain*

arjun.basandrai2022@vitstudent.ac.in

shourya.jain2022@vitstudent.ac.in

Vellore Institute of Technology

Vellore, Tamil Nadu, India

Ilanthenral K

ilanthennal.k@vit.ac.in

Vellore Institute of Technology

Vellore, Tamil Nadu, India

Abstract

Traditional resampling methods for addressing class imbalance in supervised classification typically use fixed sampling distributions, either uniformly undersampling the majority class or oversampling the minority class. These static strategies fail to account for changes in class-wise learning difficulty during the training process, which can limit the overall performance of the model.

This paper proposes an Adaptive Resampling-based Training (ART) method that periodically updates the distribution of the training data based on the class-wise performance of the model. Specifically, ART uses class-wise macro F1 scores, computed at fixed intervals, to determine the degree of resampling to be performed.

In contrast to instance-level difficulty modeling, which can be noisy and overly sensitive to outliers, ART adapts at the class level using the defined performance metric. This allows the model to incrementally shift its attention towards underperforming classes in a way that better aligns with the optimization objective.

Experimental results across diverse class-imbalanced benchmark datasets like the Pima Indians Diabetes dataset and the Yeast dataset demonstrate that ART consistently outperforms both resampling-based and algorithm-level methods, including Synthetic Minority Oversampling Technique (SMOTE), NearMiss Undersampling, and Cost-sensitive Learning on binary as well as multi-class classification tasks with varying degrees of imbalance.

In most settings, these improvements are statistically significant. On tabular datasets, gains are significant under both paired t-tests and Wilcoxon signed-rank tests ($p < 0.05$), while performance on text and image tasks remains consistently favorable. Compared to training on the original imbalanced data, ART improves macro F1 by an average of 2.64 percentage points across all tested tabular datasets. Unlike existing methods, whose performance varies by task, ART consistently delivers the strongest macro F1 score, making it a reliable and broadly effective choice for imbalanced classification problems.

CCS Concepts

• **Computing methodologies** → **Batch learning**; *Computer vision*; Natural language processing.

Keywords

Adaptive Resampling-based Training, Difficulty-aware Learning, Class Imbalance, Resampling Strategies, Supervised Classification, Data Mining, Machine Learning

1 Introduction

The highly challenging task of training classifiers on imbalanced datasets is a long-standing problem in supervised learning. In real-world applications, like fraud detection, medical diagnosis, and rare event prediction, the class distributions are often highly skewed, leading standard learning algorithms to be heavily biased towards the majority class. To mitigate this problem, many techniques have been proposed. Existing approaches include resampling-based methods, which either resample statically before the training process or dynamically while training. Static approaches like Random Over-Sampling (ROS) [8], Random Under-Sampling (RUS) [8], Synthetic Minority Oversampling Technique (SMOTE) [7], and nearmiss undersampling [23] fail to consider the changing difficulty of identifying a class as training progresses. Current dynamic approaches focus on instance-level hardness and often fail to account for imbalance in data. Other approaches are algorithmic, such as cost-sensitive learning [12], Online Hard Example Mining (OHEM) [28], and focal loss [19], which modify the loss function to assign higher costs to misclassifying or minority class examples, thereby increasing the gradient contribution from these instances during optimization. More importantly, these methods fail to consider the changing difficulty of identifying a class as training progresses. While being effective in some cases, all of these methods share common assumptions, as they either (i) treat imbalance as a static property, fixed before the training begins, (ii) focus on instance-level hardness rather than class-level, or (iii) rely on complex heuristics to assign class-specific loss weights. These assumptions ignore the fact that class difficulty evolves during learning [29, 31]. A class that initially seems difficult due to low representation may, over time, become easier to learn as the model adapts. Static correction cannot adapt to these dynamics, and often leads to overfitting on the minority class or wasting capacity by oversampling far beyond what is actually needed.

To this end, we propose ART, a resampling-based method that uses the class-wise macro F1-score as a simple heuristic for adjusting the data distribution. To the best of our knowledge, this is a novel approach that dynamically resamples data based on model performance. ART periodically monitors class-wise performance and updates the sampling distribution to emphasize underperforming classes. This class-level focus avoids the instability associated with instance-level difficulty estimation [29] and treats class difficulty as dynamic rather than static throughout training. Figure 1 shows how the sampling distribution of classes changes based on the macro F1-score as training progresses. Using a class-wise metric

*Both authors contributed equally to this research.

as a resampling heuristic offers a simpler and more robust alternative to complex fixed heuristics. Figure 2 shows how training progresses under ART. Unlike [29], which uses both resampling and a modified loss function, ART demonstrates that performance metric-based resampling alone outperforms existing methods. Also, ART utilizes a balance of performance metric-based sampling and the original dataset priors rather than completely ignoring the original data distribution. We demonstrate that ART consistently outperforms existing methods across classification tasks, achieving superior accuracy, recall, precision, and F1-scores. We also show that ART performs better than the baseline at varying levels of imbalance. Furthermore, we evaluate ART on classification tasks across tabular, image, and text datasets to demonstrate its modality-agnostic nature.

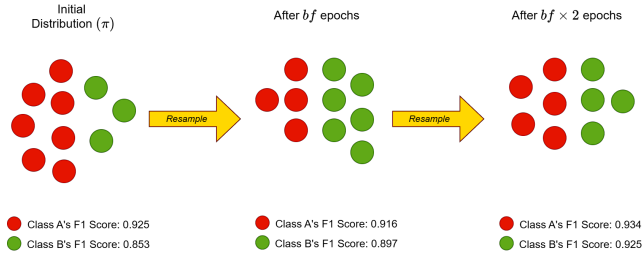


Figure 1: Adaptive resampling in ART is based on class-wise macro F1-score. The F1-score is used to estimate class difficulty, and the data distribution is updated every bf epochs to emphasize underperforming classes.

2 Related Work

Resampling-based methods: A common approach to handle class imbalance is to rebalance the data distribution before or during training. Classic techniques include ROS, which simply duplicates minority-class examples, and RUS, which deletes majority-class examples. ROS and RUS are simple resampling methods and have been shown to be surprisingly competitive on some tasks. More sophisticated oversampling methods generate synthetic examples. These include methods like SMOTE [7], which interpolates new minority examples in the feature space. Many SMOTE variants aim to focus sampling on hard or informative regions. For instance, Borderline-SMOTE [15] generates points near class boundaries, and ADASYN [16] adjusts sampling density based on local minority density. There are also some recent methods like Safe-Level-SMOTE [5] and k-means-SMOTE [11] that combine clustering or noise filtering with synthetic generation. In practice, oversampling can introduce noisy or redundant points, so hybrid methods that combine oversampling with cleaning have been proposed in [2]. For example, SMOTE-ENN and SMOTE-Tomek, as described in [3], use Edited Nearest Neighbors or Tomek-link removal to prune ambiguous samples after SMOTE. It has been shown that these hybrid methods yield well-defined class clusters and often outperform vanilla undersampling, especially when the minority class is minimal [2, 3].

In parallel, many modern variants of undersampling select the majority of examples based on distance or density. For example, the NearMiss family of methods removes the majority samples closest

to the minority class (or vice versa), and variants like NearMiss-2 pick those majority examples that lie near many minority points [23]. Such methods exploit geometric margins between classes. Other approaches cluster the data first and then undersample within clusters to preserve structure [33].

Loss-based methods: Rather than altering the data distribution, many techniques modify the learning algorithm or loss function. Classic cost-sensitive learning assigns a higher weight to the loss component of minority classes [13]. One can weigh the loss inversely by class frequency, or use a pre-specified cost matrix [12]. However, determining optimal costs can be difficult for complex models. Focal loss [19] addresses class imbalance in deep learning by changing the loss contribution of easy (well-classified) examples, thereby encouraging the model to focus on harder instances. Similarly, OHEM [28] dynamically selects the examples with the highest loss within each mini-batch and focuses training on those “hard” samples rather than the full dataset. Although OHEM originated in computer vision, the idea of mining difficult instances can be applied in any domain.

More recently proposed loss functions explicitly encode the class imbalance. For example, Label-Distribution-Aware Margin (LDAM) loss learns a per-class margin that is inversely related to class frequency, encouraging larger classification margins for minority classes [6]. Furthermore, it was shown that when LDAM is combined with a Deferred Reweighting (DRW) schedule, it outperforms standard reweighting on long-tailed image benchmarks. Their method first trains with a margin-aware loss (but without class reweighting), then fine-tunes with inverse-frequency weighting. The idea is to avoid early overfitting to minorities and give a balanced starting point before rebalancing later. Other related approaches include the “class-balanced loss” [10], which weights cross-entropy by the effective number of samples per class, and more recent margin-based softmax [26] or contrastive losses [27] tailored for imbalance. In general, these loss-based methods act at the instance level. Importantly, many of the above are static in their reweighting schedule: the class weights or sampling target is set a priori or according to a fixed curriculum, rather than being continuously updated based on model performance.

Dynamic, instance-level and curriculum methods A recent trend is to make sampling or weighting adaptive during training. Inspired by curriculum learning, some methods gradually shift the sampling distribution or loss focus over the course of learning. For example, Dynamic Curriculum Learning (DCL) [32] maintains two schedulers: a sampling scheduler and a loss scheduler. The sampling scheduler starts with an imbalanced-target distribution in early epochs (favoring the majority class) and gradually moves towards a balanced distribution. This is motivated by the observation that training too balanced too early can hurt majority-class representation. DCL shows that such a dynamic schedule yields a better trade-off between overall accuracy and balanced accuracy. Other curriculum-based methods dynamically pick which classes or instances to emphasize. For example, the model might first learn from “easy” majority examples and only later focus on the minority class (or vice versa) [4].

Techniques like self-paced learning [17] or focal loss adjust selection based on how confidently the model predicts each sample. Some recent works, like AdaSampling frameworks [34], iteratively

update example weights by model feedback, although many such methods focus on label-noise scenarios. Margin-based sampling methods, like MSYN [14], explicitly choose instances near class boundaries to improve learning when the classifier has small margins on some samples. In general, instance-level adaptive sampling contrasts with class-level rebalancing because it can upweight or downweight individual examples even within the same class.

Multi-modal Imbalanced Learning: In practice, imbalanced methods are applied across domains (vision, NLP, tabular data, etc.). Techniques like random sampling and SMOTE assume only vector inputs and have been used extensively in tabular and image datasets. Modern deep-learning loss reweighting (e.g., LDAM+DRW, focal loss) was popularized on vision tasks but extends naturally to NLP or other modalities. For instance, focal loss has been applied in text classification to handle rare classes, and cost-sensitive learning is common in medical diagnosis or fraud detection on tabular data. Class-balanced sampling and ensemble methods like Balanced Meta-Softmax [26] and LDAM+DRW have been evaluated on both image benchmarks and real-world text or tabular tasks. Moreover, some recent works explicitly benchmark multiple modalities: for example, Cui et al. [10] and Cao et al. [6] validated their class-balanced and margin-based losses on both image recognition and text classification tasks.

3 Methodology

Consider a training dataset $\mathcal{D} = \{(x_n, y_n)\}_{n=1}^N$ containing N labeled samples. Each sample consists of an input feature vector x_n from an input space \mathcal{X} and an associated class label y_n from a set of K classes. Formally:

$$\begin{aligned} x_n &\in \mathcal{X} \\ y_n &\in \{0, 1, \dots, K-1\} \end{aligned}$$

We explicitly assume the dataset exhibits significant imbalance across classes, meaning that the distribution of samples is heavily skewed, with some classes represented more frequently than others. The extent of imbalance can adversely affect predictive performance, particularly for minority classes. To characterize this imbalance quantitatively, we define the empirical class prior Π for each class i as the relative frequency of that class within the dataset:

$$\Pi_i = \frac{1}{N} \sum_{n=1}^N \mathbf{1}[y_n = i],$$

where N is the total number of samples and $\mathbf{1}[\cdot]$ is an indicator function.

Because no difficulty signal is available in the beginning, we set the class weights to a uniform vector,

$$w_i^{(0)} = \frac{1}{K}, \quad i = 0, \dots, K-1.$$

See Algorithm 1 for how these initial weights are blended with the empirical priors via convex interpolation to form the first sampling distribution.

The classification model used in this study is a parameterized function, defined by:

$$f_\theta : \mathcal{X} \rightarrow \Delta^{K-1},$$

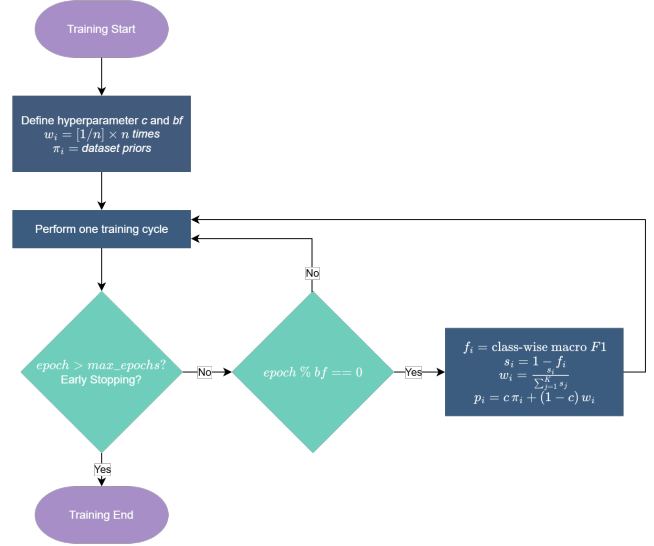


Figure 2: Overview of the training procedure in ART. The process begins with uniform initialization of class weights. Training proceeds in epochs, with periodic updates to class weights every bf epochs based on per-class macro F1-scores evaluated on a validation set.

where Δ^{K-1} denotes the $(K-1)$ -simplex, representing valid categorical probability distributions over the K classes. The model parameters, collectively denoted as θ , are optimized by minimizing the expected classification loss under a dynamically adapted sampling distribution $p \in \Delta^{K-1}$. Formally, the optimization problem is given by:

$$\hat{\theta} = \arg \min_{\theta} \sum_{i=0}^{K-1} p_i \mathbb{E}_{(x,y) \sim D_i} [L(f_\theta(x), y)]$$

where $D_i \subset D$ denotes the subset of training samples belonging to class i , and L represents a suitable classification loss function (e.g., cross-entropy loss).

3.1 Overview

The main aim of ART is to enhance model performance in classification tasks by explicitly addressing variations in predictive performance across classes. ART accomplishes this by utilizing an adaptive sampling mechanism informed directly by the current performance of the classifier, rather than relying solely on fixed empirical class frequencies. In contrast to conventional static resampling methods, ART periodically revises the sampling distribution by assessing and quantifying the classification difficulty of individual classes based on validation metrics. The algorithm for training and resampling under ART is explained in Algorithm 1. Classes identified as challenging, indicated by lower predictive performance, receive increased sampling priority. Consequently, ART systematically reallocates training resources towards improving performance on classes exhibiting greater classification complexity.

This dynamic refinement of the sampling distribution occurs iteratively at configurable intervals during the training process.

The two hyperparameters that control the behavior of this adaptive procedure are:

- (1) the *blending constant*, denoted by $c \in [0, 1]$, which controls the balance between sampling based on empirical class priors and the adaptive distribution derived from current class performance metrics;
- (2) the *boosting frequency*, denoted by $bf \in \mathbb{Z}^+$, which specifies the interval, measured in epochs, at which the sampling distribution is updated.

These hyperparameters influence how ART adjusts its sampling strategy over the course of training, and affects both the frequency and intensity of its response to class-level learning difficulty changes.

3.2 Performance-based Sampling

The ART framework periodically evaluates the current predictive performance on each class after every bf epochs. Specifically, the algorithm computes the F1-score for each class i on a held-out validation set \mathcal{V} . The class-wise difficulty score, representing how challenging each class is for the current model state, is then defined as:

$$s_i = 1 - f_i,$$

where f_i is the class-wise F1-score obtained from the validation set.

These computed difficulty scores reflect the inverse performance relationship and hence, emphasize classes with poor predictive performance. To create a valid probability distribution from these difficulty scores, we normalize them across all classes, resulting in a performance-based sampling weights given by:

$$w_i = \frac{s_i}{\sum_{j=1}^K s_j}, \quad i = 1, \dots, K.$$

This normalization guarantees that classes with lower predictive performance will have proportionally higher sampling probabilities, thereby allowing the training algorithm to put greater emphasis towards classes that are currently more difficult to learn. As the model improves on previously challenging classes, the sampling distribution adjusts dynamically, thereby redistributing the focus towards other underperforming classes.

3.3 Blending with Class Priors

To ensure stable training, ART does not rely entirely on performance-based adaptive sampling distributions. Instead, it creates a blended sampling distribution by performing a convex interpolation between the empirical class prior distribution Π_i and the adaptive performance-based distribution w_i . Formally, the blended sampling probability for each class i is defined by:

$$p_i = c \Pi_i + (1 - c) w_i, \quad i = 1, \dots, K,$$

where the blending factor $c \in [0, 1]$ explicitly controls the relative weighting between the empirical prior and adaptive distributions. A higher value of c prioritizes sampling according to the original empirical class priors, and a lower value of c prioritizes the adaptive distribution by shifting sampling more towards the currently underperforming classes.

Algorithm 1: Adaptive Resampling-based Training (ART)

Input: Training set $\mathcal{D} = \{(x_n, y_n)\}_{n=1}^N$, empirical prior Π , blending factor $c \in [0, 1]$, boost frequency $bf \in \mathbb{Z}^+$, total epochs E

Output: Trained model parameters $\hat{\theta}$

Initialisation

Initialise model f_θ (parameters θ);

Set *uniform initial class weights*:

$$w_i \leftarrow \frac{1}{K}, \quad i = 0, \dots, K - 1;$$

Set *initial sampling distribution*: $p_i \leftarrow c \Pi_i + (1 - c) w_i$;

for epoch $\leftarrow 1$ to E do

Draw minibatches from \mathcal{D} according to p ;

Update θ by gradient descent on the minibatch loss;

if epoch mod $bf = 0$ then

Evaluate per-class F1 scores f_i on the validation set;

Compute difficulties $s_i \leftarrow 1 - f_i$;

Normalise to new adaptive weights $w_i \leftarrow \frac{s_i}{\sum_{j=0}^{K-1} s_j}$;

Update sampling distribution $p_i \leftarrow c \Pi_i + (1 - c) w_i$;

return $\hat{\theta} \leftarrow \theta$

Our convex combination strategy is essential, particularly during the early stages of training, as some classes may temporarily exhibit near-zero performance-based weights ($w_i \approx 0$). Without blending, these classes risk temporary exclusion from the training process, leading to unintended behavior during loss computation.

4 Experiments

4.1 Experimental Setup

We evaluate ART against a broad suite of existing methods across five datasets commonly used for imbalanced classification tasks: Pima Indians Diabetes [30], Yeast [24], Red Wine Quality [9], a custom long-tailed version of MNIST [18] (MNIST-LT), and a synthetically imbalanced IMDB sentiment classification dataset [22] (IMDB-Custom). MNIST-LT was prepared by taking an imbalance factor of 0.01 and the number of samples for majority class were taken as 1500. All samples were chosen randomly in accordance to the imbalance factor. IMDB-Custom dataset was prepared by transforming the reviews into embedding vectors using all-MiniLM-L6-v2 [25] by sentence-transformers. Then an arbitrary imbalance ratio of 7 was chosen and samples were randomly chosen from the data in accordance to it. Pima Indians Diabetes dataset is a binary classification dataset with an imbalance ratio of 1.86. Red Wine Quality dataset is a multi-class classification dataset with 6 classes. It has an imbalance ratios ranging from 1.06 to 68.1 in comparison to the class with most instances. Yeast dataset is a multi-class classification dataset with 9 classes, with imbalance ratios ranging from 1.08 to 23.15 in comparison to the class with highest number of instances. These datasets encompass both binary and multi-class classification scenarios and vary substantially in terms of class imbalance, feature dimensionality, and input modality (tabular, image, and text).

Each dataset is split into 70% for training, 15% for validation, and 15% for testing. Continuous features in the tabular datasets are standardized using Z-Score Normalization. Bayesian hyperparameter optimization is performed for each method using Optuna’s TPE sampler [1]. For tabular datasets, we conduct $25 \times n$ trials, where n is the number of hyperparameters (capped at 4 using $n = \min(\text{no. of hyperparameters}, 4)$). For MNIST-LT and IMDB-Custom, we use $5 \times n$ trials due to the computational constraints. All models are trained using the AdamW optimizer [21] with a cosine annealing learning rate scheduler [20]. Early stopping is applied with a patience of 10 epochs, based on the loss on the validation set.

We use consistent model architectures across experiments: a lightweight feedforward network for tabular data and IMDB-Custom, and a compact CNN for image classification. Since Nearmiss has multiple variations, we use the best variation for each dataset based on hyperparameter optimization. Model-specific configurations are held constant across all baselines to ensure fair comparison.

4.2 Compared Methods

We benchmark ART against a range of resampling-based and algorithm-level methods for handling class imbalance:

Resampling-based Methods:

- No Imbalance Handling (Baseline)
- ROS
- RUS
- SMOTE
- MSMOTE
- NearMiss Undersampling

Loss-based Methods:

- Cost-Sensitive Learning
- Focal Loss
- OHEM
- LDAM + DRW

4.3 Evaluation Protocol

Each method is evaluated using 20 random seeds to ensure robustness. We report the following:

- Mean and standard deviation of macro-F1 scores on the held-out test set.
- Paired t -test and Wilcoxon signed-rank test to assess the statistical significance of ART compared to each baseline.
- Average rank of each method across the 20 runs.

More information about measures taken to ensure fairness and reproducibility in results can be found in Appendix B

4.4 Test Results

Table 1 presents the macro-F1 scores across all five datasets.

ART achieves the highest macro-F1 scores across all datasets. ART consistently performs well on other metrics, which can be seen in Table 1 and Appendix C. Below, we provide dataset-specific observations:

Pima Indians Diabetes. ART achieves a consistent improvement over strong baselines, demonstrating its effectiveness in moderately imbalanced binary classification tasks.

Yeast. This dataset poses a significant challenge due to its multi-class nature. ART demonstrates clear superiority, likely due to its adaptive class-wise attention mechanism.

Red Wine Quality. Given its severe class imbalance, this dataset emphasizes ART’s capacity to handle challenging, skewed distributions effectively.

MNIST-LT. ART maintains stable performance, highlighting its robustness in long-tailed image classification scenarios.

IMDb-Custom. ART demonstrates competitive performance, illustrating the flexibility of adaptive resampling techniques in text classification.

To verify that ART’s improvements are not due to random seed variation, we test each baseline against ART with both a paired t -test and a two-sided Wilcoxon signed-rank test over the same 20 seeds used in the main experiments. Appendix –A reports the resulting p-values, where entries below 0.05 indicate a statistically significant advantage for ART. We consistently achieve p-value < 0.05 against most methods, indicating significant performance gains when using ART compared to other methods.

4.5 Ablation Studies

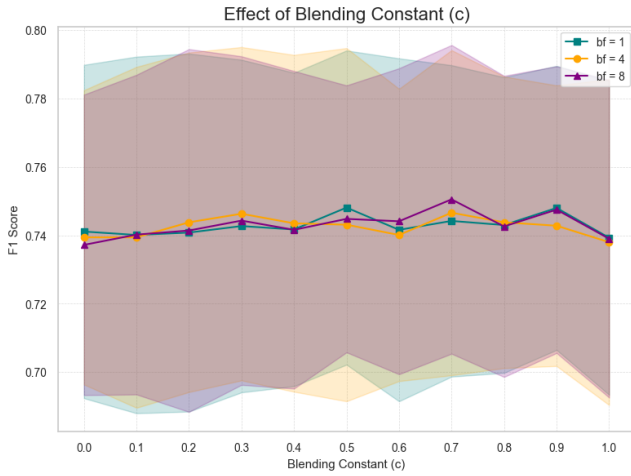
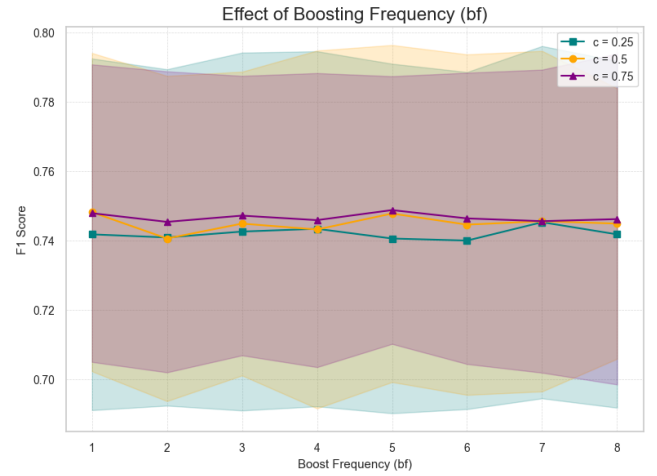
To evaluate the robustness and sensitivity of ART to its key hyperparameters and design choices, we conducted a series of ablation studies. Due to computational constraints, these experiments were carried out on the Pima Indians Diabetes dataset, which provides a reasonable balance between class imbalance, binary classification, and fast convergence. While the results are specific to this dataset, the trends, particularly ART’s stability and consistent performance across different settings, are expected to generalize, given that the method does not rely on any modality-specific assumptions. Future work can expand these studies to include a wider range of datasets and modalities.

4.5.1 Effect of the Blending Constant c . The blending constant $c \in [0, 1]$ controls the weight assigned to the static class prior versus the dynamic class-wise performance when creating the sampling distribution. We evaluated ART’s performance using $c = 0.0, 0.1, 0.2, 0.3, 0.4, 0.5, 0.6, 0.7, 0.8, 0.9, 1.0$ using three different values of the hyperparameter $bf = 1, 4, 8$. These values cover the low, mid and high range of values of the bf for the dataset used. Figure 3 shows the value of macro F1-score on these different c values. Performance remained stable across all c values, indicating that ART is not sensitive to this parameter. Hence, a mid-range value like $c = 0.5$ offers a reliable default setting.

4.5.2 Effect of Boost Frequency bf . The boost frequency bf controls how often the class distribution is updated during training. We evaluated ART with $bf = 1, 2, 3, 4, 5, 6, 7, 8, 9, 10$, covering frequent, moderate, and infrequent updates. Each configuration was tested with three values of the blending constant $c = 0.25, 0.5, 0.75$, covering low, medium and high values. As shown in Figure 4, performance remained consistent across all combinations, suggesting that ART does not require frequent updates to maintain effectiveness. Hence, this reduces the need for extensive hyperparameter tuning in practice.

Table 1: Performance comparison of ART and existing methods on Macro-F1 score (mean \pm std over 20 seeds).

Method	Pima	Yeast	Red Wine	MNIST-LT	IMDb-Custom
Baseline	0.7371 \pm 0.0502	0.5152 \pm 0.0531	0.3126 \pm 0.0533	0.8736 \pm 0.0470	0.7258 \pm 0.0171
ROS	0.7483 \pm 0.0457	0.4727 \pm 0.0419	0.3303 \pm 0.0508	0.8792 \pm 0.0407	0.7166 \pm 0.0211
RUS	0.7529 \pm 0.0441	0.4286 \pm 0.0501	0.1928 \pm 0.0368	0.6714 \pm 0.0368	0.6839 \pm 0.0214
SMOTE	0.7500 \pm 0.0443	0.4829 \pm 0.0408	0.3281 \pm 0.0487	—	—
MSMOTE	0.7479 \pm 0.0482	0.5008 \pm 0.0417	0.2993 \pm 0.0381	—	—
NearMiss	0.7566 \pm 0.0398	0.3767 \pm 0.0521	0.1169 \pm 0.0392	—	—
Cost-Sensitive Learning	0.7442 \pm 0.0480	0.3912 \pm 0.0689	0.2790 \pm 0.0266	0.8808 \pm 0.0468	0.722 \pm 0.0174
Focal Loss	0.7414 \pm 0.0487	0.5094 \pm 0.0548	0.3193 \pm 0.0512	0.8716 \pm 0.0344	0.7247 \pm 0.0168
OHEM	0.7344 \pm 0.0475	0.5007 \pm 0.0380	0.2697 \pm 0.0297	0.8879 \pm 0.0393	0.7197 \pm 0.0171
LDAM+DRW	0.7559 \pm 0.0489	0.5073 \pm 0.0521	0.2878 \pm 0.0246	0.8464 \pm 0.0588	0.7025 \pm 0.0269
ART (Ours)	0.7631 \pm 0.0498	0.5306 \pm 0.0432	0.3506 \pm 0.0613	0.8848 \pm 0.0359	0.7296 \pm 0.0165

**Figure 3: Comparison of ART performance over different blending constant (c) where c is a hyperparameter. Results show ART is insensitive to the choice of c and requires minimal hyperparameter optimization.****Figure 4: Comparison of performance of ART across varying boosting frequency (bf) values while keeping all other hyperparameters constant. Experiments over varying c values show performance is insensitive to choice of boosting frequency.**

4.5.3 Effect of Model Width. To examine ART's behavior under different model capacities, we varied the initial model width (d) from 16 to 512 in powers of two while keeping other model architecture choices constant. As shown in Figure 5, both ART and the baseline improve with increased width, but ART consistently outperforms the baseline at all sizes. For instance, ART achieves an F1 score of 0.7419 ± 0.0454 at width 64, while the baseline requires width 256 to reach a comparable score of 0.7394 ± 0.0458 . In this case, ART matches performance using a model that is four times smaller. It also exhibits lower standard deviations across widths. This suggests that ART trains more stably across random seeds. It also performs well even when the model is small. This makes ART a good choice for low-resource settings where model capacity is limited.

4.5.4 Performance Across Imbalance Ratios. To assess ART's robustness under varying degrees of class imbalance, we generated

synthetic variants of the Pima Indians Diabetes dataset with imbalance ratios ranging from 2 to 50. We then compared ART to a baseline model trained without any imbalance mitigation.

As shown in Figure 6, ART consistently outperforms the baseline across all imbalance ratios. While both methods experience a decline in macro-F1 as imbalance severity increases, ART demonstrates significantly better stability. For instance, at an imbalance ratio of 10, ART achieves a macro-F1 of approximately 0.68, whereas the baseline drops to around 0.56. Even at extreme imbalance levels, ART maintains a notable advantage, highlighting its ability to adapt sampling in response to increasing class difficulty.

5 Conclusion

We conclude by highlighting key results, discussing current limitations, and outlining promising directions for future research.

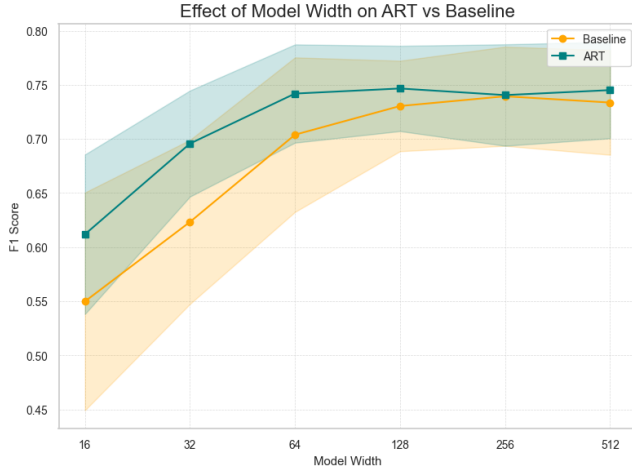


Figure 5: Comparison of baseline and ART performance over different model width. Other model architecture choices and training hyperparameters were kept constant.

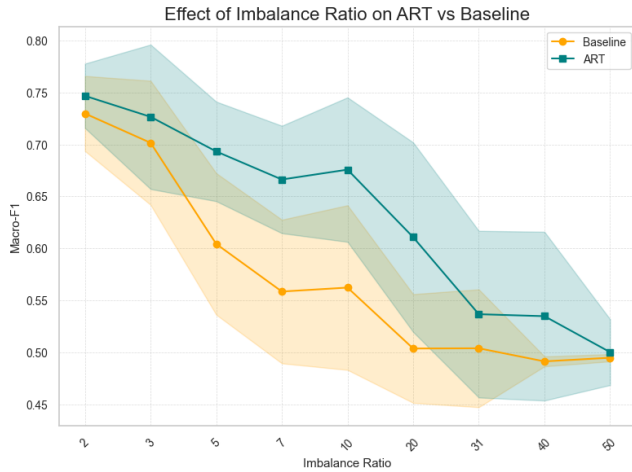


Figure 6: ART maintains higher performance than Baseline at most imbalance levels, with both methods showing a decline as imbalance increases. Shaded areas indicate variability across runs.

5.1 Results

Across five benchmark datasets covering tabular, image, and text modalities, ART consistently achieved the strongest macro-F1 scores, outperforming every method we tested. On the Pima, Yeast, and Red Wine datasets, it improved over the best competitor by 1.0–3.8 percentage points and increased the mean macro-F1 across all tabular datasets by 2.64 percentage points. These gains were statistically significant according to paired t -tests and Wilcoxon signed-rank tests ($p < 0.05$). ART also maintained its advantage on the long-tailed MNIST-LT and the synthetically imbalanced IMDb-Custom dataset, confirming its modality-agnostic design. Notably, ART

matched or exceeded baseline performance even when the underlying model’s width was reduced by a factor of four, confirming that it can maintain high performance under limited computational resources.

5.2 Limitations

ART assumes an *epoch-based* training loop that (i) computes batch-wise losses, (ii) aggregates gradients, and (iii) evaluates class-wise metrics on a validation set at regular intervals. Thus, it applies well to models trained with stochastic gradient descent (e.g. MLPs, and CNNs) but is unsuitable for non-iterative learners, like decision trees, or k-NN. In addition, computing class-wise F1 every b epochs incurs overhead proportional to the validation-set size; for very large datasets, this cost may be non-trivial unless subsampling is employed.

5.3 Future Work

Three directions look especially promising:

- (1) **Hybrid sampling.** Trying various methods for dynamic class-level rebalancing in ART could provide better performance as compared to using simple random oversampling and undersampling.
- (2) **Broader model classes.** We plan to evaluate ART on large language models and also assess its performance in standard logistic regression pipelines.
- (3) **New modalities.** Applying ART to imbalanced audio classification task would test its adaptability to high-rate time-series data where class difficulty can change rapidly during training.

Together, these avenues can deepen our understanding of ART and further widen its applicability in modern machine-learning pipelines.

References

- [1] Takuya Akiba, Shotaro Sano, Takeru Yanase, Takuya Ohta, and Masanori Koyama. 2019. Optuna: A next-generation hyperparameter optimization framework. In *Proceedings of the 25th ACM SIGKDD International Conference on Knowledge Discovery & Data Mining*. ACM, 2623–2631.
- [2] Gustavo Batista, Ronaldo Prati, and Maria-Carolina Monard. 2004. A Study of the Behavior of Several Methods for Balancing machine Learning Training Data. *SIGKDD Explorations* 6 (06 2004), 20–29. <https://doi.org/10.1145/1007730.1007735>
- [3] Gustavo E. A. P. A. Batista, Ronaldo C. Prati, and Maria Carolina Monard. 2004. A study of the behavior of several methods for balancing machine learning training data. *SIGKDD Explor. Newsl.* 6, 1 (June 2004), 20–29. <https://doi.org/10.1145/1007730.1007735>
- [4] Yoshua Bengio, Jérôme Louradour, Ronan Collobert, and Jason Weston. 2009. Curriculum learning. In *Proceedings of the 26th Annual International Conference on Machine Learning* (Montreal, Quebec, Canada) (ICML ’09). Association for Computing Machinery, New York, NY, USA, 41–48. <https://doi.org/10.1145/1553374.1553380>
- [5] Chumphol Bunkhumpornpat, Krung Sinapiromsaran, and Chidchanok Lursinsap. 2009. Safe-Level-SMOTE: Safe-Level-Synthetic Minority Over-Sampling TEchnique for Handling the Class Imbalanced Problem. In *Advances in Knowledge Discovery and Data Mining*, Thanaruk Theeramunkong, Boonserm Kijsirikul, Nick Cercone, and Tu-Bao Ho (Eds.). Springer Berlin Heidelberg, Berlin, Heidelberg, 475–482.
- [6] Kaidi Cao, Colin Wei, Adrien Gaidon, Nikos Arachiga, and Tengyu Ma. 2019. Learning Imbalanced Datasets with Label-Distribution-Aware Margin Loss. *arXiv:1906.07413 [cs.LG]* <https://arxiv.org/abs/1906.07413>
- [7] N. V. Chawla, K. W. Bowyer, L. O. Hall, and W. P. Kegelmeyer. 2002. SMOTE: Synthetic Minority Over-sampling Technique. *Journal of Artificial Intelligence Research* 16 (June 2002), 321–357. <https://doi.org/10.1613/jair.953>
- [8] Wuxing Chen, Kaixiang Yang, Zhiwen Yu, Yifan Shi, and C. L. Philip Chen. 2024. A survey on imbalanced learning: latest research, applications and future directions.

- Artificial Intelligence Review* 57, 6 (2024), 137. <https://doi.org/10.1007/s10462-024-10759-6>
- [9] Paulo Cortez, Antonio Cerdeira, Fernando Almeida, Telmo Matos, and Jose Reis. 2009. Wine Quality Data Set (Red Variant). <https://www.kaggle.com/datasets/uciml/red-wine-quality-cortez-et-al-2009>. Based on: P. Cortez, A. Cerdeira, F. Almeida, T. Matos, J. Reis. "Modeling wine preferences by data mining from physicochemical properties," *Decision Support Systems*, Elsevier, 47(4):547-553, 2009.
 - [10] Yin Cui, Menglin Jia, Tsung-Yi Lin, Yang Song, and Serge Belongie. 2019. Class-Balanced Loss Based on Effective Number of Samples. In *Proceedings of the IEEE/CVF Conference on Computer Vision and Pattern Recognition (CVPR)*.
 - [11] Georgios Douzas, Fernando Bacao, and Felix Last. 2018. Improving imbalanced learning through a heuristic oversampling method based on k-means and SMOTE. *Information Sciences* 465 (Oct. 2018), 1–20. <https://doi.org/10.1016/j.ins.2018.06.056>
 - [12] Charles Elkan. 2001. The Foundations of Cost-Sensitive Learning. *Proceedings of the Seventeenth International Conference on Artificial Intelligence: 4-10 August 2001; Seattle 1* (05 2001).
 - [13] Charles Elkan. 2001. The foundations of cost-sensitive learning. In *Proceedings of the 17th International Joint Conference on Artificial Intelligence - Volume 2* (Seattle, WA, USA) (*IJCAI'01*). Morgan Kaufmann Publishers Inc., San Francisco, CA, USA, 973–978.
 - [14] Eric Fan, Ke Tang, and Thomas Weise. 2011. Margin-Based Over-Sampling Method for Learning from Imbalanced Datasets, Vol. 6635. 309–320. https://doi.org/10.1007/978-3-642-20847-8_26
 - [15] Hui Han, Wen-Yuan Wang, and Bing-Huan Mao. 2005. Borderline-SMOTE: A New Over-Sampling Method in Imbalanced Data Sets Learning. In *Advances in Intelligent Computing*, De-Shuang Huang, Xiao-Ping Zhang, and Guang-Bin Huang (Eds.). Springer Berlin Heidelberg, Berlin, Heidelberg, 878–887.
 - [16] Haibo He, Yang Bai, Edwardo A. Garcia, and Shutao Li. 2008. ADASYN: Adaptive synthetic sampling approach for imbalanced learning. In *2008 IEEE International Joint Conference on Neural Networks (IEEE World Congress on Computational Intelligence)*. 1322–1328. <https://doi.org/10.1109/IJCNN.2008.4633969>
 - [17] M. Kumar, Benjamin Packer, and Daphne Koller. 2010. Self-Paced Learning for Latent Variable Models. In *Advances in Neural Information Processing Systems*, J. Lafferty, C. Williams, J. Shawe-Taylor, R. Zemel, and A. Culotta (Eds.), Vol. 23. Curran Associates, Inc. https://proceedings.neurips.cc/paper_files/paper/2010/file/e57c6b956a6521b28495f2886ca0977a-Paper.pdf
 - [18] Yann LeCun, Léon Bottou, Yoshua Bengio, and Patrick Haffner. 1998. Gradient-based learning applied to document recognition. *Proc. IEEE* 86, 11 (1998), 2278–2324.
 - [19] Tsung-Yi Lin, Priya Goyal, Ross Girshick, Kaiming He, and Piotr Dollár. 2018. Focal Loss for Dense Object Detection. arXiv:1708.02002 [cs.CV] <https://arxiv.org/abs/1708.02002>
 - [20] Ilya Loshchilov and Frank Hutter. 2017. SGDR: Stochastic Gradient Descent with Warm Restarts. arXiv:1608.03983 [cs.LG] <https://arxiv.org/abs/1608.03983>
 - [21] Ilya Loshchilov and Frank Hutter. 2019. Decoupled Weight Decay Regularization. arXiv:1711.05101 [cs.LG] <https://arxiv.org/abs/1711.05101>
 - [22] Andrew L. Maas, Raymond E. Daly, Peter T. Pham, Dan Huang, Andrew Y. Ng, and Christopher Potts. 2011. IMDB Dataset of 50K Movie Reviews. <https://www.kaggle.com/datasets/lakshmi25npathi/imdb-dataset-of-50k-movie-reviews>. Based on: Maas, Andrew L., Daly, Raymond E., Pham, Peter T., Huang, Dan, Ng, Andrew Y., and Potts, Christopher. "Learning Word Vectors for Sentiment Analysis," *Proceedings of the 49th Annual Meeting of the Association for Computational Linguistics (ACL 2011)*, pages 142–150..
 - [23] Inderjeet Mani. 2003. kNN Approach to Unbalanced Data Distributions: A Case Study Involving Information Extraction. In *Proceedings of Workshop on Learning from Imbalanced Datasets*.
 - [24] Kenta Nakai. 1991. Yeast. UCI Machine Learning Repository. DOI: <https://doi.org/10.24432/C5KG68>.
 - [25] Nils Reimers and Iryna Gurevych. 2021. all-MiniLM-L6-v2. <https://huggingface.co/sentence-transformers/all-MiniLM-L6-v2>. Based on: Wang et al., MiniLM: Deep Self-Attention Distillation for Task-Agnostic Compression of Pre-Trained Transformers, in *Advances in Neural Information Processing Systems (NeurIPS)* 2020. <https://arxiv.org/abs/2002.10957>.
 - [26] Jiawei Ren, Cunjun Yu, Shunan Sheng, Xiao Ma, Haiyu Zhao, Shuai Yi, and Hongsheng Li. 2020. Balanced Meta-Softmax for Long-Tailed Visual Recognition. arXiv:2007.10740 [cs.LG] <https://arxiv.org/abs/2007.10740>
 - [27] Joshua Robinson, Ching-Yao Chuang, Suvrit Sra, and Stefanie Jegelka. 2021. Contrastive Learning with Hard Negative Samples. arXiv:2010.04592 [cs.LG] <https://arxiv.org/abs/2010.04592>
 - [28] Abhinav Shrivastava, Abhinav Gupta, and Ross Girshick. 2016. Training Region-based Object Detectors with Online Hard Example Mining. arXiv:1604.03540 [cs.CV] <https://arxiv.org/abs/1604.03540>
 - [29] Saptarshi Sinha, Hiroki Ohashi, and Katsuyuki Nakamura. 2022. Class-Difficulty Based Methods for Long-Tailed Visual Recognition. *International Journal of Computer Vision* 130, 10 (Aug. 2022), 2517–2531. <https://doi.org/10.1007/s11263-022-01643-3>
 - [30] J.W. Smith, J.E. Everhart, W.C. Dickson, W.C. Knowler, and R.S. Johannes. 1988. Pima Indians Diabetes Database. <https://www.kaggle.com/datasets/uciml/pima-indians-diabetes-database>. National Institute of Diabetes and Digestive and Kidney Diseases.
 - [31] Mariya Toneva, Alessandro Sordani, Remi Tachet des Combes, Adam Trischler, Yoshua Bengio, and Geoffrey J. Gordon. 2019. An Empirical Study of Example Forgetting during Deep Neural Network Learning. arXiv:1812.05159 [cs.LG] <https://arxiv.org/abs/1812.05159>
 - [32] Yiru Wang, Weihao Gan, Jie Yang, Wei Wu, and Junjie Yan. 2019. Dynamic Curriculum Learning for Imbalanced Data Classification. arXiv:1901.06783 [cs.CV] <https://arxiv.org/abs/1901.06783>
 - [33] Show-Jane Yen and Yue-Shi Lee. 2006. Cluster-Based sampling approaches to imbalanced data distributions. In *Proceedings of the 8th International Conference on Data Warehousing and Knowledge Discovery (Krakow, Poland) (DaWaK'06)*. Springer-Verlag, Berlin, Heidelberg, 427–436. https://doi.org/10.1007/11823728_41
 - [34] Xin-Yu Zhang, Le Zhang, Zao-Yi Zheng, Yun Liu, Jia-Wang Bian, and Ming-Ming Cheng. 2019. AdaSample: Adaptive Sampling of Hard Positives for Descriptor Learning. arXiv:1911.12110 [cs.CV] <https://arxiv.org/abs/1911.12110>

Appendix

A Statistical Significance Tests

Table 2: Pima Dataset: p-values (ART vs. baselines)

Method	Paired t-test	Wilcoxon test
Baseline	0.0001	0.0003
ROS	0.0089	0.0141
RUS	0.0846	0.0642
SMOTE	0.0107	0.0023
MSMOTE	0.0087	0.0124
NearMiss	0.3070	0.1327
Cost-Sensitive	0.0018	0.0032
Focal Loss	0.0014	0.0038
OHEM	0.0005	0.0006
LDAM+DRW	0.1188	0.1231

Table 3: Yeast Dataset: p-values (ART vs. baselines)

Method	Paired t-test	Wilcoxon test
Baseline	0.1432	0.1893
ROS	0.0000	0.0000
RUS	0.0000	0.0000
SMOTE	0.0000	0.0000
MSMOTE	0.0012	0.0025
NearMiss	0.0000	0.0000
Cost-Sensitive	0.0000	0.0000
Focal Loss	0.0324	0.0266
LDAM+DRW	0.0253	0.0266

Table 4: Red Wine Dataset: p-values (ART vs. baselines)

Method	Paired t-test	Wilcoxon test
Baseline	0.0293	0.0153
ROS	0.2397	0.3683
RUS	0.0000	0.0000
SMOTE	0.1246	0.2305
MSMOTE	0.0081	0.0064
NearMiss	0.0000	0.0000
Cost-Sensitive	0.0003	0.0003
Focal Loss	0.0633	0.0583
OHEM	0.0000	0.0000
LDAM+DRW	0.0003	0.0001

B Reproducibility Details

To facilitate exact replication of our results, we provide below the fixed random-seed list, hardware configuration, and software environment used for every experiment in Section 4.

Table 5: MNIST-LT Dataset: p-values (ART vs. baselines)

Method	Paired t-test	Wilcoxon test
Baseline	0.1851	0.3683
ROS	0.4923	0.5706
RUS	0.0000	0.0000
Cost-Sensitive	0.7052	0.8695
Focal Loss	0.0874	0.0825
LDAM+DRW	0.0058	0.0073

Table 6: IMDb-Custom Dataset: p-values (ART vs. baselines)

Method	Paired t-test	Wilcoxon test
Baseline	0.4482	0.3884
ROS	0.0278	0.0318
RUS	0.0000	0.0000
Cost-Sensitive	0.1714	0.1671
Focal Loss	0.3244	0.4330
LDAM+DRW	0.0001	0.0007

B.1 Random Seeds

All runs were executed with the following 20 integer seeds, applied uniformly to NumPy, PyTorch, and (where applicable) CUDA. We used the following seeds for running our tests: 1834, 8993, 412, 4523, 182, 41921, 53178, 4536, 89, 101172, 3812, 76459, 21734, 5601, 14923, 32871, 982, 61435, 23490, 7711. Metrics for each method are averaged over all 20 seeds.

B.2 Hardware

- **GPU.** All training was performed on a single NVIDIA Tesla P100 (16 GB) provided by Kaggle notebooks.
- **CPU.** 1 × Intel Xeon (model 85, Skylake) @ 2.00 GHz, 4 vCPUs (2 cores × 2 threads), little-endian, AVX-512 capable, 38.5 MiB shared L3.
- **RAM.** 31 GiB system RAM (free -g reports ≈22 GiB free and ≈7 GiB cached at notebook start).

All experiments ran inside a standard Kaggle notebook container

B.3 Determinism Controls

Before every run, we invoked the helper below to seed all relevant RNGs and disable non-deterministic cuDNN paths:

```
def seed_env(SEED):
    random.seed(SEED)
    np.random.seed(SEED)
    torch.manual_seed(SEED)
    if torch.cuda.is_available():
        torch.cuda.manual_seed(SEED)
        torch.cuda.manual_seed_all(SEED)
    torch.backends.cudnn.deterministic = True
    torch.backends.cudnn.benchmark = False
```

These details should allow the readers to reproduce the results reported in Tables 1 and 2–6.

C Performance Metrics

We demonstrate the performance of ART against existing methods on various metrics. See Table 7 for performance on accuracy, Table 8

for performance on precision and Table 9 for performance on recall.

Table 7: Performance comparison of ART and existing methods on Accuracy (mean \pm std over 20 seeds).

Method	Pima	Yeast	Red Wine	MNIST-LT	IMDb-Custom
Baseline	0.7636 \pm 0.0408	0.5853 \pm 0.0254	0.6100 \pm 0.0261	0.9777 \pm 0.0060	0.9218 \pm 0.0061
ROS	0.7633 \pm 0.0412	0.5396 \pm 0.0377	0.5789 \pm 0.0398	0.9766 \pm 0.0119	0.9157 \pm 0.0084
RUS	0.7672 \pm 0.0412	0.4536 \pm 0.0473	0.2881 \pm 0.0677	0.8587 \pm 0.0315	0.8491 \pm 0.0215
SMOTE	0.7663 \pm 0.0402	0.5340 \pm 0.0342	0.5527 \pm 0.0408	—	—
MSMOTE	0.7603 \pm 0.0442	0.5835 \pm 0.0268	0.5968 \pm 0.0389	—	—
NearMiss	0.7698 \pm 0.0363	0.3804 \pm 0.0577	0.1625 \pm 0.0776	—	—
Cost-Sensitive Learning	0.7573 \pm 0.0443	0.4806 \pm 0.0361	0.5577 \pm 0.0394	0.9726 \pm 0.0139	0.9049 \pm 0.0133
Focal Loss	0.7668 \pm 0.0402	0.5779 \pm 0.0324	0.6035 \pm 0.0302	0.9766 \pm 0.0063	0.9212 \pm 0.0078
OHEM	0.7599 \pm 0.0402	0.5774 \pm 0.0230	0.5862 \pm 0.0373	0.9778 \pm 0.0060	0.9214 \pm 0.0061
LDAM+DRW	0.7728 \pm 0.0423	0.5768 \pm 0.0354	0.6120 \pm 0.0300	0.9674 \pm 0.0170	0.8884 \pm 0.0239
ART (Ours)	0.7758 \pm 0.0502	0.5914 \pm 0.0332	0.5737 \pm 0.0372	0.9770 \pm 0.0065	0.9083 \pm 0.0183

Table 8: Performance comparison of ART and existing methods on Precision (mean \pm std over 20 seeds).

Method	Pima	Yeast	Red Wine	MNIST-LT	IMDb-Custom
Baseline	0.7495 \pm 0.0515	0.5565 \pm 0.0732	0.3251 \pm 0.0729	0.8976 \pm 0.0491	0.7762 \pm 0.0333
ROS	0.7482 \pm 0.0478	0.4708 \pm 0.0522	0.3393 \pm 0.0622	0.9062 \pm 0.0468	0.7474 \pm 0.0277
RUS	0.7544 \pm 0.0493	0.4350 \pm 0.0618	0.2375 \pm 0.0344	0.6606 \pm 0.0324	0.6540 \pm 0.0179
SMOTE	0.7518 \pm 0.0469	0.4794 \pm 0.0545	0.3369 \pm 0.0657	—	—
MSMOTE	0.7478 \pm 0.0496	0.5372 \pm 0.0607	0.3094 \pm 0.0358	—	—
NearMiss	0.7566 \pm 0.0427	0.3893 \pm 0.0566	0.2094 \pm 0.0479	—	—
Cost-Sensitive Learning	0.7457 \pm 0.0512	0.4811 \pm 0.1131	0.2879 \pm 0.0302	0.8951 \pm 0.0594	0.7234 \pm 0.0318
Focal Loss	0.7525 \pm 0.0507	0.5591 \pm 0.0742	0.3312 \pm 0.0725	0.9034 \pm 0.0386	0.7744 \pm 0.0332
OHEM	0.7459 \pm 0.0505	0.5436 \pm 0.0484	0.2973 \pm 0.0340	0.9134 \pm 0.0465	0.7746 \pm 0.0270
LDAM+DRW	0.7515 \pm 0.0508	0.5490 \pm 0.0597	0.3392 \pm 0.0490	0.9112 \pm 0.0470	0.7522 \pm 0.0236
ART (Ours)	0.7673 \pm 0.0519	0.5644 \pm 0.0595	0.3583 \pm 0.0645	0.9068 \pm 0.0437	0.7341 \pm 0.0330

Table 9: Performance comparison of ART and existing methods on Recall (mean \pm std over 20 seeds).

Method	Pima	Yeast	Red Wine	MNIST-LT	IMDb-Custom
Baseline	0.7331 \pm 0.0496	0.5229 \pm 0.0521	0.3136 \pm 0.0489	0.8643 \pm 0.0475	0.6969 \pm 0.0227
ROS	0.7530 \pm 0.0451	0.5275 \pm 0.0474	0.3504 \pm 0.0655	0.8706 \pm 0.0356	0.6958 \pm 0.0224
RUS	0.7584 \pm 0.0416	0.4903 \pm 0.0488	0.2999 \pm 0.0991	0.7714 \pm 0.0510	0.7777 \pm 0.0208
SMOTE	0.7532 \pm 0.0425	0.5476 \pm 0.0439	0.3619 \pm 0.0707	—	—
MSMOTE	0.7566 \pm 0.0462	0.5126 \pm 0.0375	0.3108 \pm 0.0507	—	—
NearMiss	0.7635 \pm 0.0386	0.4732 \pm 0.0636	0.3028 \pm 0.0879	—	—
Cost-Sensitive Learning	0.7525 \pm 0.0463	0.4326 \pm 0.0670	0.2972 \pm 0.0265	0.8822 \pm 0.0407	0.7318 \pm 0.0357
Focal Loss	0.7374 \pm 0.0482	0.5176 \pm 0.0499	0.3214 \pm 0.0460	0.8613 \pm 0.0360	0.6964 \pm 0.0234
OHEM	0.7314 \pm 0.0470	0.5097 \pm 0.0450	0.2728 \pm 0.0266	0.8778 \pm 0.0388	0.6885 \pm 0.0223
LDAM	0.7346 \pm 0.0505	0.5367 \pm 0.0473	0.3250 \pm 0.0424	0.8794 \pm 0.0451	0.7042 \pm 0.0227
DRW	0.7581 \pm 0.0491	0.5325 \pm 0.0532	0.2908 \pm 0.0223	0.8591 \pm 0.0455	0.7282 \pm 0.0254
ART (Ours)	0.7703 \pm 0.0428	0.5458 \pm 0.0485	0.3783 \pm 0.0767	0.8777 \pm 0.0385	0.7349 \pm 0.0291